A first-principles study of electronic and magnetic properties of 4d transition metals doped in Wurtzite GaN for spintronics applications

A First-Principles Study of Electronic and Magnetic Properties of 4d Transition Metals Doped in Wurtzite GaN for Spintronics Applications

Omkar A. Shilkar[1,2], Rajendra Adhikari[3], Subrahmanyam Sappati[4,5], Shreya Godi[1,2] and Ashish M. Desai[1*]

[1*]Department of Physics, Parvatibai Chowgule College of Arts and Science, Margao, 403602, Goa, India.
[2]School of Physical and Applied Sciences, Goa University, 403206, Goa, India.
[3]Department of Physics, Kathmandu University, Dhulikhel, 45200, Nepal.
[4]Department of Pharmaceutical Technology and Biochemistry, Gdańsk University of Technology, Gdańsk, 80-233, Poland.
[5]BioTechMed Center, Gdańsk University of Technology, Gdańsk, 80-233, Poland.

*Corresponding author(s). E-mail(s): amd006@chowgules.ac.in;

Abstract

We studied the electronic and magnetic properties of wurtzite GaN (w-GaN) doped with different concentrations of the 4d transition metal ions Nb, Mo, and Ru. We incorporated spin-polarized plane-wave density functional theory within an ultrasoft pseudopotential formalism. The 4d transition metals were doped at different geometrical sites to determine the geometry with the lowest total energy and the one that induced the largest magnetization. A spin-spin interaction study was performed to determine whether the doped compound was ferromagnetic or antiferromagnetic. The origin of magnetization in the transition-metal-doped w-GaN compounds is due to the p-d hybridization of the nitrogen and 4d transition metals. From the bulk modulus results, we inferred that the structural integrity is preserved under compressive loads

after doping w-GaN with these 4d transition metal ions. Our results indicate that these compounds can be used in spintronic applications.

Keywords: GaN, Density functional theory, Electronic properties, Magnetic properties, Spintronic devices

1 Introduction

Gallium nitride (GaN) is a mechanically stable wide-bandgap semiconductor with potential applications in high-speed switching transistors, light-emitting diodes, photodetectors, and solar cells. Owing to their higher breakdown strength and ability to conduct electrons more efficiently leading to lower heat generation, GaN-based power devices are more efficient and compact than their Si counterparts [1]. Moreover, due to its higher electron mobility, GaN is a suitable option to replace Si-based devices because of its ability to operate at higher frequencies and sustain higher temperatures than Si and SiC [2]. The crystal structure of GaN, which is thermodynamically the most stable and has the lowest total energy, is the wurtzite structure (w-GaN) [3]

Dilute magnetic semiconductors (DMSs), which are formed by introducing transition metals into intrinsic nonmagnetic semiconductors, have received considerable attention for their possible applications in semiconductor spintronics. Unlike conventional volatile DRAM, spintronic devices store information bits using magnetic spin states instead of storing electrons. This method of data storage makes spintronic memory devices non-volatile. In general, dilute magnetic semiconductors show ferromagnetism after being doped with transition metals [4–11]. Room temperature ferromagnetism has been observed in several studies, which is a necessary condition for a material to be applied in spintronics, this can be achieved by doping w-GaN with group B transition metals [12–16]. Recently, antiferromagnets and ferrimagnets have also been reported to be useful for various applications in spintronic devices [17, 18]. Xiong et. al. [17] in their study described the applications of antiferromagnets in AFM-based memories. Zhang et. al. [18] discussed the various class of ferrimagnets including oxides and alloys and their applications in storage and computing devices.

Extensive studies have been carried out to determine electronic and magnetic properties of materials by doping 3d transition metals in GaN [19–32]. Comparatively few studies have reported the effects of 4d transition metals doped in GaN [33–38]. Garcia et. al. [33] and Osuch et. al. [34] studied the magnetic properties of GaN doped with Ag and Pd respectively. The authors concluded that doping Ag and Pd into GaN induced ferromagnetic ordering in the compound. Compounds $Ag_{0.0625}Ga_{0.9375}N$ and $Pd_{0.0625}Ga_{0.9375}N$ possess magnetic moments of 1.8 μ_B and 1.3 μ_B per supercell, respectively. Moreover, magnetization is induced in the doped compound $Pd_{0.0625}Ga_{0.9375}N$ even though Pd is nonmagnetic in its natural phase. The authors [33, 34] suggested

that including 4d metals as dopants in semiconductors may overcome the technological limitations in producing dilute magnetic semiconductors, and that these compounds can be important candidates for spintronics applications. Therefore, it is of interest to study alternative 4d series elements doped in wide-gap semiconductors that could give rise to potential candidates for spintronic applications.

In this study, we performed first-principles calculations to determine the electronic and magnetic properties of w-GaN doped with Nb, Mo, and Ru. A spin-spin interaction study was carried out to determine the ground-state total energy difference between ferromagnetic and antiferromagnetic spin systems. Furthermore, formation energies were calculated to confirm the thermodynamic stability of the doped compounds.
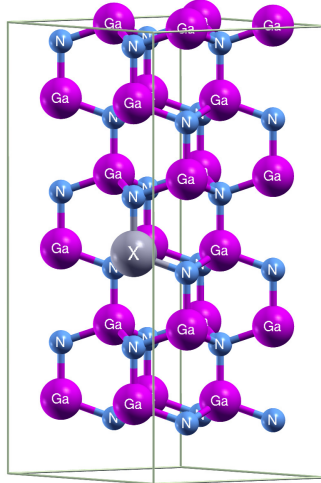
2 Computational Methods

First-principles calculations were carried out using spin-polarized, pseudopotential density functional theory [39, 40] as implemented in the plane-wave based Quantum ESPRESSO simulation package [41–43]. We adopted ultrasoft pseudopotentials to describe electron-ion interactions, with the Perdew-Burke-Ernzerhof (PBE) [44] parametrization of the generalized gradient approximation (GGA) for the electron-electron exchange-correlation potential energy for all the calculations. The electron wave function was expanded in plane waves with a kinetic energy cutoff of 816 eV, and the Brillouin zone was sampled in the special Monkhorst-Pack scheme [45] using a gamma-centered $8 \times 8 \times 8$ k-point mesh for the unit cell. The Marzari-Vanderbilt smearing technique [46] was used with a smearing width of 0.01 Ry. Using these parameters, we achieved total energy convergence better than 0.0001 meV for all calculations.

For structure optimization, each structure was optimized until the maximum stress was less than 1 Kbar and the Hellman-Feynman force was less than 10^{-4} Ry/Å or 1 meV/Å. GaN in the wurtzite crystal structure is characterized by three lattice parameters: $a = b = 3.216$ Å and $c = 5.24$ Å. We calculated the electronic structure of 4d transition metal doped GaN using a 48-atom $2a \times 2b \times 3c$ supercell to investigate the magnetic properties of $Ga_{1-x}TM_xN$ doped with $x = 0.042, 0.083$. Fig. 1 depicts the compound representing a concentration of 4.2%.

For the compound representing a concentration of 8.3%, two 4d transition metals were doped in the pristine supercell of w-GaN by TM = Ru, Nb and Mo at six different geometrical sites within w-GaN to determine the structure that has the lowest total energy and the structure that induces the largest magnetization. Fig. 2a shows the structure with energetically the most stable doping arrangement (doping configuration C_1) for the two Nb and Ru-doped w-GaN supercells, and Fig. 2b shows the lowest energy doping configuration (C_2) for the two Mo-doped w-GaN supercell. Fig. 2c depicts the structure that induces the largest magnetization (doping configuration C_3) for all three TMs = Nb, Mo, and Ru doped into w-GaN. The other structures of two 4d

transition metals replacing two Ga atoms at different geometrical sites in the w-GaN supercell are shown in the Supplementary Information. Furthermore, the ground state energies were calculated and compared to determine whether the dopants induced ferromagnetism or antiferromagnetism in w-GaN.
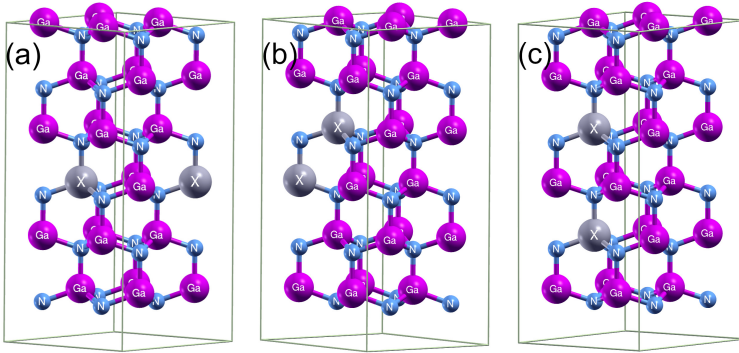

Fig. 1 Supercell structure of $Ga_{0.958}Nb_{0.042}N$ (TM = Nb, Mo and Ru). The magenta, light blue, and gray atoms represent Ga, N, and TM dopants respectively.

3 Results and Discussion

3.1 Structural Properties

The volume optimization of GaN, $Ga_{0.958}Nb_{0.042}N$ and $Ga_{0.917}TM_{0.083}N$ with TM = Nb, Mo, and Ru was performed to determine its structural properties. Self-consistent field calculations were performed for several values of lattice constants above and below the optimum lattice constant. The total energy was calculated for each lattice constant. The bulk modulus, total energy, and lattice constant were obtained by fitting the data to the Birch-Murnaghan equation of state. The Birch-Murnaghan equation of state is given as [47]

$$E(V) = E_0 + \frac{9V_0B_0}{16}\left[\left\{\left(\frac{V_0}{V}\right)^{2/3} - 1\right\}^2 B_0' + \left\{\left(\frac{V_0}{V}\right)^{2/3} - 1\right\}^2 \left\{6 - 4\left(\frac{V_0}{V}\right)^{2/3}\right\}\right],$$

(1)

Fig. 2 Supercell of $Ga_{0.917}Nb_{0.083}N$ (TM = Nb, Mo and Ru) (a) Ground state structure of Nb- and Ru-doped systems (doping configuration C_1) (b) ground state of Mo-doped system (doping configuration C_2), and (c) highest magnetization inducing structure (doping configuration C_3) for Nb-, Ru-, and Mo-doped systems. The magenta, light blue, and gray spheres represent Ga, N, and TM dopants, respectively.

where V_0 is the reference volume, V is the deformed volume, E_0 is the ground state energy, B_0 is the bulk modulus and B_0' is the derivative of the bulk modulus with respect to pressure.
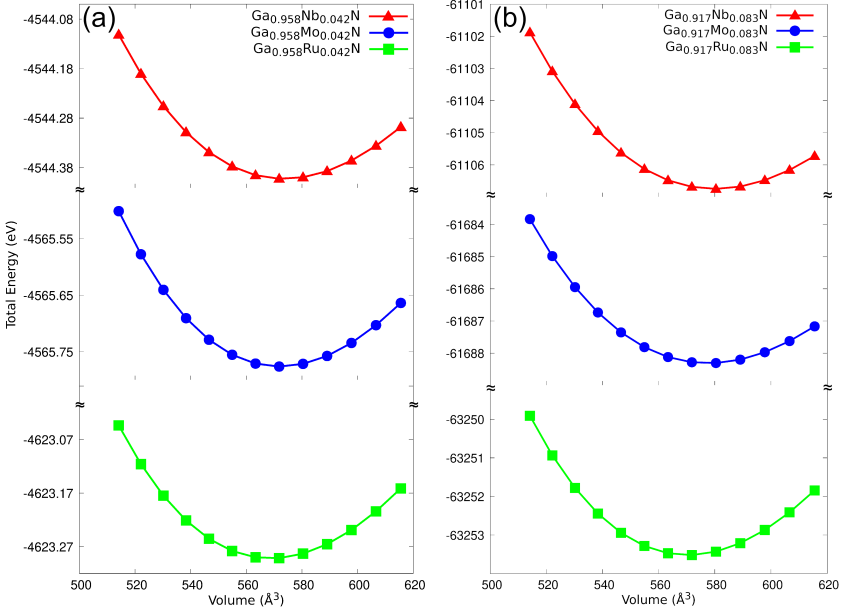
Table 1 Lattice constants and bulk modulus of pristine GaN, $Ga_{0.958}TM_{0.042}N$ and $Ga_{0.917}TM_{0.083}N$ with (TM = Nb, Mo and Ru) in the wurtzite structure.

Compound $Ga_{1-x}TM_xN$	a (Å)	c (Å)	Bulk Modulus (GPa)
GaN(Pristine)	3.213	5.235	172.0
	3.189[1]	5.185[1]	173.0[2]
$Ga_{0.958}Nb_{0.042}N$	6.468	15.785	168.8
$Ga_{0.958}Ru_{0.042}N$	6.451	15.731	171.1
$Ga_{0.958}Mo_{0.042}N$	6.461	15.773	168.3
$Ga_{0.917}Nb_{0.083}N$	6.501	15.826	167.6
$Ga_{0.917}Ru_{0.083}N$	6.461	15.765	172.3
$Ga_{0.917}Mo_{0.083}N$	6.486	15.821	166.0

[1]Experimental Value of lattice constants [48]
[2]Experimental Value of Bulk Modulus [49]

The bulk modulus and lattice constant values obtained from the Birch-Murnaghan fit of w-GaN are listed in Table 1. The value of the bulk modulus $B_0 = 172$ GPa and lattice constants for the ground state of w-GaN, $a = 3.213$ Å and $c = 5.235$ Å, are in accordance with the experimental value of bulk modulus $B_0 = 173$ GPa reported in the literature [48] and values of lattice constants $a = 3.189$ Å and $c = 5.185$ Å reported in the literature [49]. From Table 1 we infer that the hardness is preserved for GaN doped with Mo, Nb, and Ru because the values obtained for the bulk modulus of the

Fig. 3 Variation in total energy with the volume of (a) $Ga_{0.958}TM_{0.042}N$ (TM = Nb, Mo and Ru) (b) $Ga_{0.917}TM_{0.083}N$ (TM = Nb, Mo and Ru)

doped compounds are close to the value of pristine w-GaN. The plots of the total energy versus volume for $Ga_{0.958}TM_{0.042}N$ and $Ga_{0.917}TM_{0.083}N$ with TM = Nb, Mo, and Ru are shown in Fig. 3. The formation energies of Mo-, Nb-, and Ru-doped w-GaN compounds were calculated to determine their energy stability. The expression to calculate the formation energy is given as [12]

$$E_F = E_{tot} - E_{ref} - mE_{TM} + mE_{Ga}, \qquad (2)$$

where E_{tot} is the energy of the transition-metal-doped GaN compounds, E_{ref} is the energy of the pristine w-GaN, E_{TM} is the energy of the dopant, E_{Ga} is the energy of the Ga atom and m is the number of transition metals that replace Ga atoms in w-GaN. The formation energies of the $Ga_{0.958}TM_{0.042}N$ compounds are listed in Table 2 and those of the $Ga_{0.917}TM_{0.083}N$ compounds for all doping configurations C_1, C_2 and C_3 are listed in Table 3. From the formation energies of the doped GaN compounds, we can infer that these ternary compounds are thermodynamically stable and can be grown experimentally. Furthermore, compounds formed by doping Nb into GaN are energetically the most favorable because they have the most negative formation energies.

3.2 Electronic properties

All three 4d transition elements, Nb, Mo, and Ru, generated magnetic moments for $Ga_{0.958}TM_{0.042}N$ (TM = Nb, Mo, and Ru) compounds, that is, at a concentration of 4.8%. The induced magnetization values are presented in Table 2. Among the ground state doping configurations, C_1 for $Ga_{0.917}TM_{0.083}N$ (TM = Nb and Ru) and C_2 for $Ga_{0.917}Mo_{0.083}N$ only Mo generates a magnetic moment in w-GaN. In addition, the C_2 doping configuration of the $Ga_{0.917}Mo_{0.083}N$ compound exhibited a stable ferromagnetic state. This result agrees with that reported by Xiao et. al. [35]. In their study, room-temperature ferromagnetism was observed in a Mo-doped GaN ML. The configuration C_1 of w-GaN doped with either Nb or Ru was found to be nonmagnetic. The values of the induced magnetization and the total energy difference for the ferromagnetic and antiferromagnetic states are listed in Table 3. Furthermore, all three elements, Nb, Mo, and Ru, generated magnetic moments in the configuration structure C_3 of the compound $Ga_{0.917}TM_{0.083}N$ (TM = Nb, Mo, and Ru). The values of the induced magnetization and total energy difference between the ferromagnetic and antiferromagnetic states for this structure are listed in Table 3. We infer from the total energy difference between the ferromagnetic and antiferromagnetic states, given in Table 3, that the doping configuration C_3 doped with Mo or Ru atoms shows a stable ferromagnetic state. The C_3 configuration of $Ga_{0.917}Nb_{0.083}N$ compound favors antiferromagnetic ordering in the system, however, due to asymmetry in the Nb-N bond lengths at the two dopant sites, there is a residual, net non-zero magnetization of 0.14 μ_B, as shown in Table 3. Our results for Ru-doped GaN agree with those reported by Latif et. al [36]. They concluded that the ferromagnetic state is more favorable than the antiferromagnetic state in Ru-doped c-GaN. A similar result was reported by Ghosal et. al. [37] in their study of Ru doped in zincblende ZnS.

Table 2 Calculated total magnetization and formation energies (E_F) of $Ga_{0.958}TM_{0.042}N$ compound with TM = Nb, Mo and Ru.
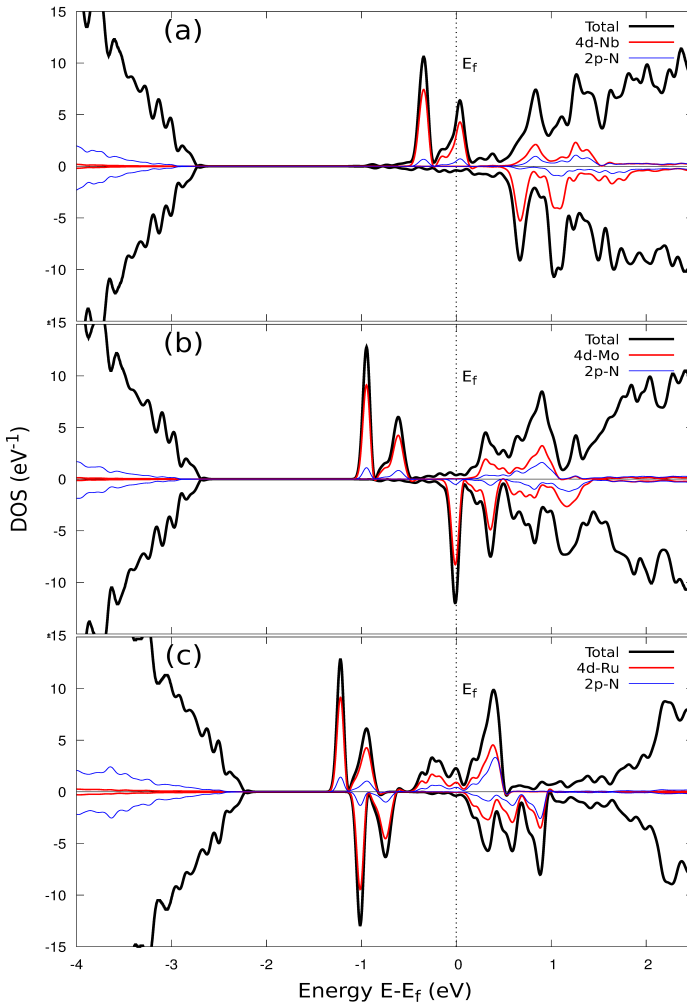
Compound $Ga_{1-x}TM_xN$	Magnetization (μ_B)	E_F (eV)
GaN(Pristine)	0	-
$Ga_{0.958}Nb_{0.042}N$	1.57	-2.54
$Ga_{0.958}Ru_{0.042}N$	0.91	-0.10
$Ga_{0.958}Mo_{0.042}N$	1.43	-0.32

The spin-polarized total and partial density of states were calculated to determine the electronic structures of the compounds. The total and partial density of states for the $Ga_{.958}TM_{0.042}N$ (TM = Nb, Mo and Ru) compounds are shown in Fig. 4. The Fermi level was set to zero while plotting the density of states. In all the figures, the density of states plots is asymmetric, which suggests that magnetization is induced by the presence of unpaired spins in all doped systems.
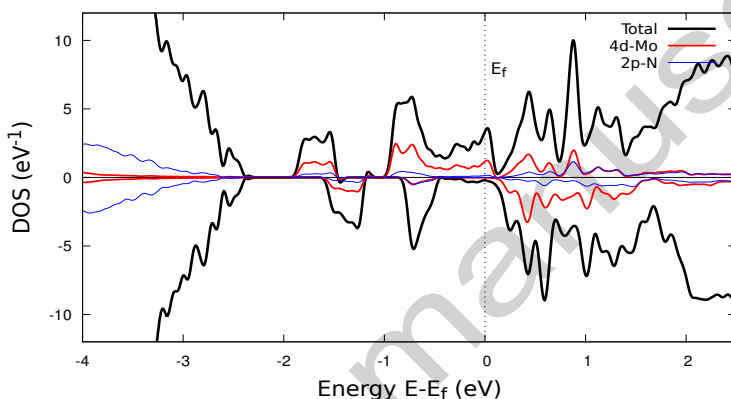
Table 3 The calculated total magnetization, total energy difference ($\Delta E = E_{\text{FM}} - E_{\text{AFM}}$), ground state configurations (non-magnetic (NM), ferromagnetic (F), and antiferromagnetic (AF)), and formation energies (E_{F}) for the ground state of $Ga_{0.958}TM_{0.042}N$ compound with TM = Nb, Mo and Ru for doping configurations C_1, C_2 and C_3.

Doping Config.	Compound $Ga_{1-x}TM_xN$	Magnetization (μ_B) F	AF	ΔE (meV)	Ground state	E_F (eV)
C_1	$Ga_{0.917}Nb_{0.083}N$	0.2	0	0.26	NM	-6.17
	$Ga_{0.917}Ru_{0.083}N$	0	0	-0.125	NM	-1.76
C_2	$Ga_{0.917}Mo_{0.083}N$	1.78	1.15	-1657.59	F	-2.07
C_3	$Ga_{0.917}Nb_{0.083}N$	3.45	0.14	2.80	AF	-5.00
	$Ga_{0.917}Ru_{0.083}N$	1.93	0.01	-320.13	F	-0.22
	$Ga_{0.917}Mo_{0.083}N$	2.66	0.11	-0.11	F	-0.53

Fig. 4 Calculated total and partial density of states for (a) $Ga_{0.958}Nb_{0.042}N$, (b) $Ga_{0.958}Mo_{0.042}N$, and (c) $Ga_{0.958}Ru_{0.042}N$. Contributions of one transition metal atom and four neighboring nitrogen atoms were considered. The vertical dashed line denotes the Fermi level, which is shifted to zero.

The total and partial DOS plots of ground state structure (doping configuration C_1) of the compound $Ga_{0.917}TM_{0.083}N$ (TM = Nb and Ru) are presented in the Supplementary Information. Because the PDOS plots of Nb and Ru doped in w-GaN for configuration C_1 are symmetric, we infer that there is no induced magnetization for this doping configuration. This result is in agreement with the zero-calculated magnetization value for this structure. The PDOS plot of ground state structure (doping configuration C_2) for $Ga_{0.917}Mo_{0.083}N$ compound is shown in Fig. 5. The PDOS plot of Mo-doped w-GaN is asymmetric which suggests a nonzero magnetic moment for the structure.
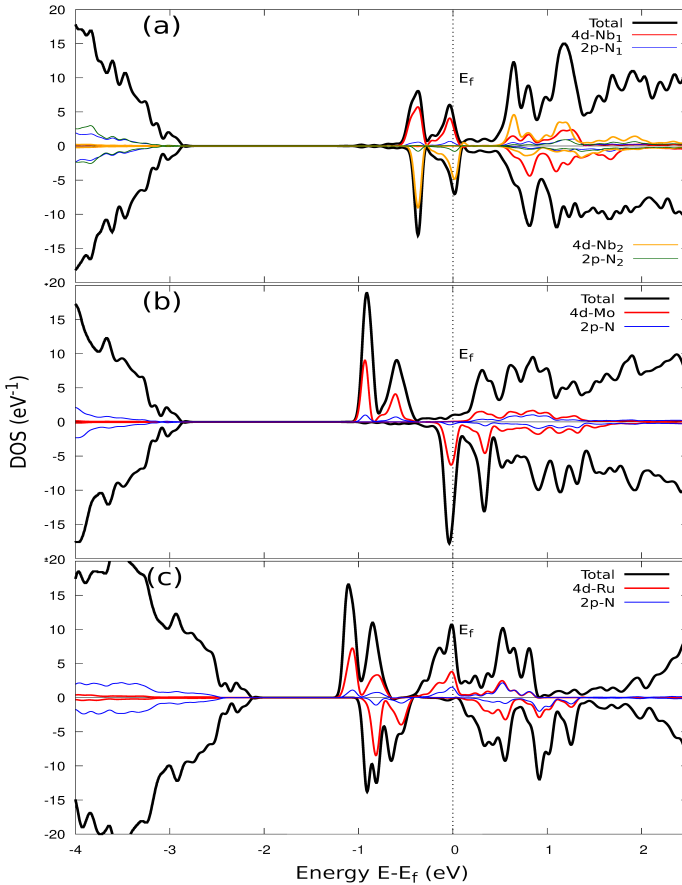

Fig. 5 Calculated total and partial density of states for the lowest energy structure of $Ga_{0.917}Mo_{0.083}N$ (doping configuration C_2). Contributions of one Mo atom and four neighboring nitrogen atoms were considered. The vertical dashed line denotes the Fermi level, which is carried to zero.

Fig. 6 shows the calculated total and partial DOS plot of the structure that induces the largest magnetization (doping configuration C_3) for all three TMs = Nb, Mo, and Ru doped into w-GaN. We infer from Fig. 6a, that despite Nb-doped GaN exhibiting an antiferromagnetic spin configuration, the PDOS plot is asymmetric which is in agreement with the non-zero net magnetization. This is due to slightly different geometry at the two dopant sites due to local perturbations in the bond length of Nb-N. The structure with the bond length of Nb-N is shown in the Supplementary Information. Hence the doping configuration C_3 of the compound $Ga_{0.958}Nb_{0.042}N$ appears to be ferrimagnetic.

From Fig. 6b and 6c, we infer that the main contribution to the down-spin density in the DOS plot of Mo doped w-GaN is due to the 4d-Mo state and the main contribution to the up-spin density in the DOS plot of Ru doped w-GaN is due to the 4d-Ru state. In addition, from these plots, we conclude that there is a small contribution from the 2p-N states crossing the Fermi level to the

up-spin density in Ru-doped w-GaN and the down-spin density in Mo-doped w-GaN. Hybridization occurred between the 4d-Ru and 4d-Mo states of the metallic dopants and the 2p states of the nitrogen atom close to the Fermi level. Hence, we conclude that the magnetization in the transition-metal-doped w-GaN compounds is due to the p-d hybridization of the nitrogen and transition metal ions. Similar results were reported by Espitia et. al., [12], and Doumi et. al., [50], in their study of the electronic properties of 3d transition metals (Ti, V, Cr, Mn, and Fe) doped in GaN compounds in the zincblende phase.

Fig. 6 Calculated total and partial density of states for highest magnetization inducing structure (doping configuration C_3) for (a) $Ga_{0.917}Nb_{0.083}N$ (2p-N_1 and 2p-N_2 represent the contribution from four nitrogen atoms neighboring to Nb_1 and Nb_2 dopant sites respectively), (b) $Ga_{0.917}Mo_{0.083}N$, and (c) $Ga_{0.917}Ru_{0.083}N$. The vertical dashed line denotes the Fermi level, which is carried to zero.

4 Conclusions

First-principle spin-polarized calculations were performed to study the electronic and magnetic properties of GaN doped with 4d transition metals (Nb, Mo, and Ru) in the wurtzite phase. All three 4d-transition elements generate magnetic moments in the $Ga_{0.958}TM_{0.042}N$ (TM = Nb, Mo, and Ru) compounds. Among the lowest-energy doping arrangements, configurations C_1 of $Ga_{0.917}TM_{0.083}N$ (TM = Nb and Ru) and configuration C_2 of $Ga_{0.917}Mo_{0.083}N$, only Mo generated a magnetic moment in w-GaN. Among the two dopant structures that induce the largest magnetization (configuration C_3), the ferromagnetic spin configuration of Mo and Ru doped into w-GaN is more energetically favorable, whereas the antiferromagnetic spin configuration is favored in the Nb-doped w-GaN compound. Furthermore, the doping configuration C_3 of compound $Ga_{0.917}Nb_{0.083}N$ is ferrimagnetic because of the small nonzero net magnetization. From the calculation of the partial density of states, we infer that the main contribution to the total magnetic moment induced in compounds $Ga_{0.958}TM_{0.042}N$ and $Ga_{0.917}TM_{.083}N$ (TM = Nb, Mo, and Ru) originates mainly from the transition metal atoms. In addition, magnetization is generated by hybridization of the p-d states of nitrogen and 4d-transition metal atoms. We envisage that these compounds will be promising materials for spintronic applications.

Supplementary Information. The figures of two 4d transition metals (Nb, Mo, and Ru) replacing two Ga atoms at different geometrical sites in the w-GaN supercell and the corresponding values of the total energy and magnetization are provided in the Supplementary Information. The total and partial DOS plots of the doping configuration C_1 of $Ga_{0.917}TM_{0.083}N$ (TM = Nb and Ru) and configuration C_3 of $Ga_{0.917}Nb_{0.083}N$ structure with the bond length of Nb-N are also shown in the Supplementary Information.

Declarations:

Ethical Approval. Not applicable.

Competing interests. The authors declare that they have no competing interests.

12

References

[1] Y. Zhong, J. Zhang, S. Wu, L. Jia, X. Yang, Y. Liu, Y. Zhang, Q. Sun, A review on the GaN-on-Si power electronic devices, *Fundamental Research*, 2(3) (2022) 462-475.

[2] T. J. Flack, B. N. Pushpakaran, S. B. Bayne, GaN Technology for Power Electronic Applications: A Review, *Journal of Electronic Materials*, 45(6) (2016) 2673-2682.

[3] P. Bhattacharya, R. Fornari, H. Kamimura, Comprehensive Semiconductor Science and Technology, 2011.

[4] H. Kalita, M. Bhushan, L. R. Singh, A comprehensive review on theoretical concepts, types and applications of magnetic semiconductors, *Materials Science and Engineering: B*, 288 (2023) 116201.

[5] N. Seña, A. Dussan, F. Mesa, E. Casta no, R. González-Hernández, Electronic structure and magnetism of Mn-doped GaSb for spintronic applications: A DFT study, *Journal of Applied Physics*, 120(5) (2016) 051704.

[6] S. Roy, H. Luitel, D. Sanyal, Magnetic properties of transition metal doped SnO_2: A detailed Theoretical study, *Computational Condensed Matter*, 21 (2019) e00393.

[7] A. Alsaad, Structural, electronic and magnetic properties of Fe, Co, Mn-doped GaN and ZnO diluted magnetic semiconductors, *Physica B: Condensed Matter*, 440 (2014) 1-9.

[8] C. Liu, F. Yun, H. Morkoc, Ferromagnetism of ZnO and GaN: A Review, *Journal of Materials Science: Materials in Electronics*, 16(9) (2005) 555-597.

[9] B. Seipel, R. Erni, A. Gupta, C. Li, F. J. Owens, K. V. Rao, N. D. Browning, P. Moeck, Structural and ferromagnetic properties of Cu-doped GaN, *Journal of materials research*, 22(5) (2007) 1396-1405.

[10] H. Luitel, S. Roy, D. Sanyal, Ab-initio calculation of the magnetic properties of P and As doped SnO_2, *Computational Condensed Matter*, 14 (2018) 36-39.

[11] J. Li, H. Liu, Theoretical research of diluted magnetic semiconductors: GaN monolayer doped with transition metal atoms, *Superlattices and Microstructures*, 120 (2018) 382-388.

[12] M. J. Espitia R, O. S. Parra, C.O. López, Electronic and magnetic behavior of transition metal-doped cubic gallium nitride: first-principles calculations, *Journal of Magnetism and Magnetic Materials*, 451 (2018) 295-299.

[13] H. Luitel, P. Chettri, A. Tiwari, D. Sanyal, Experimental and first principle study of room temperature ferromagnetism in carbon-doped rutile TiO_2, Materials Research Bulletin, 110 (2019) 13-17.

[14] V. G. Saravade, C. H. Ferguson, A. Ghods, C. Zhou, I. T. Ferguson, Room Temperature Ferromagnetism in Gadolinium-doped Gallium Nitride, *MRS Advances*, 3(3) (2018) 159-164.

[15] S. Dhar, L. Pérez, O. Brandt, A. Trampert, K. H. Ploog, J. Keller, B. Beschoten, Gd-doped GaN: A very dilute ferromagnetic semiconductor with a Curie temperature above 300 K, *Physical Review B*, 72(24) (2005) 245203.

[16] H. Pan, J. B. Yi, L. Shen, R. Q. Wu, J. H. Yang, J. Y. Lin, Y. P. Feng, J. Ding, L. H. Van, J. H. Yin, Room-Temperature ferromagnetism in carbon-doped ZnO, *Physical review letters*, 99(12) (2007) 127201.

[17] D. Xiong, Y. Jiang, K. Shi, A. Du, Y. Yao, Z. Guo, D. Zhu, K. Cao, S. Peng, W. Cai, D. Zhu, W. Zhao, Antiferromagnetic spintronics: An overview and outlook, *Fundamental Research*, 2 (4) (2022) 522-534.

[18] Y. Zhang, X. Feng, Z. Zheng, Z. Zhang, K. Lin, X. Sun, G. Wang, J. Wang, J. Wei, P. Vallobra, Y. He, Z. Wang, L. Chen, K. Zhang, Y. Xu, W. Zhao, Ferrimagnets for spintronic devices: From materials to applications, *Applied Physics Reviews*, 10 (2023) 011301.

[19] Romanudhin, W. A. E. Prabowo, F. Fathurrahman, A. Melati, H. K. Dipojono, A first principle study of the electronic structures of transition metal doped GaN for diluted magnetic semiconductor applications, *Procedia Engineering*, 170 (2017) 124–130.

[20] M. H. Eisa, Electronic structure and optical properties of Cd co-doped wurtzite GaN exposed from first principles study, *Results in Physics*, 13 (2019) 102330.

[21] N. Tandon, G. P. Das, A. Kshirsagar, Electronic structure of GaN codoped with Mn and Cr, *Physical Review B*, 77(20), 205206, 2008.

[22] G. P. Das, B. K. Rao, P. Jena, Ferromagnetism In Mn-Doped GaN: From clusters to crystals, *Physical Review B*, 68(3) (2003) 035207.

[23] M. Shakil, Abrar Husain, M. Zafar, Shabir Ahmad, M.I. Khan, M. Kashif, Masood, Abdul Majid, Ferromagnetism in GaN doped with transition metals and rare-earth elements: A review, *Chinese Journal of Physics*, 56(4) (2018) 1570-1577.

[24] Y. Guo, M. Chen, Z. Guo, X. Yan, First-principles calculations for magnetic properties of Mn-doped GaN nanotubes, *Physics Letters A*, 372(15) (2008) 2688-2691.

[25] G. Yao, G. Fan, S. Zheng, J. Ma, J. Chen, D. Zhou, S. Li, Y. Zhang, S. Su, First-principles analysis on V-doped GaN, *Optical Materials*, 34(9) (2012) 1593-1597.

[26] J. Rufinus, Magnetic properties of M-doped (M = Ti, V, or Cr) GaN clusters, *Journal of Magnetism and Magnetic Materials*, 310(2) (2007) 1666–1668.

[27] H. Qin, X. Luan, C. Feng, D. Yanga, G. Zhang, Mechanical, Thermodynamic, and Electronic Properties of Wurtzite and Zinc-Blende GaN Crystals,*Materials*, 10(12) (2017) 1419.

[28] Y. Li, W. Fan, H. Sun, X. Cheng, P. Li, X. Zhao, M. Jiang, Nitrogen vacancy and ferromagnetism in Cr-doped GaN: First-principles calculation, *Journal of Solid State Chemistry*, 183(11) (2010) 2662-2668.

[29] R. G. Hernandez, W. L Perez, F. Fajardo, J. A. Rodriguez, Pressure effects on the electronic and magnetic properties of $Ga_xV_{1-x}N$ compounds: Ab-initio study, *Materials Science and Engineering B*, 163(3) (2009) 190-193.

[30] J. Kang, K. J. Chang, The electronic and magnetic properties of Mn-doped GaN, *Physica B:Condensed Matter*, 376 (2006) 635-638.

[31] B. Belhadji, L. Bergqvist, R. Zeller, P. H. Dederichs, K Sato, H. K.-Yoshida, Trends of exchange interactions in dilute magnetic semiconductors, *Journal of Physics Condensed Matter*, 19(43) (2007) 436227.

[32] T. Dietl, H. Ohno, Dilute ferromagnetic semiconductors: Physics and spintronic structures, Reviews of Modern Physics, 86(1) (2014) 187.

[33] A. G. García, W. L. Pérez, R. G. Hernández, Ab initio calculations of magnetic properties of Ag-doped GaN, *Computational Materials Science*, 55 (2012) 171-174.

[34] K. Osuch, E. B. Lombardi, L. Adamowicz, Palladium in GaN: A 4d metal ordering ferromagnetically in a semiconductor, *Physical Review B*, 71(16) (2005) 165213.

[35] G. Xiao, L. Wang, Q. Rong, H. Xu, W. Xiao, A comparative study on magnetic properties of Mo doped AlN, GaN and InN monolayers from first-principles, *Physica B: Condensed Matter*, 524 (2017) 47-52.

[36] A. Latif, M. Khan, Z. Kanwal, I. Majeed, M. Saleem, N. Usmani, J. Ahmad, Z. Mustansar, H. Ullah, Investigating effect of different Hubbard values on the electronic structure, magnetic and optical properties of Ru-doped GaN, *Computational Condensed Matter*, 29 (2021) e00608.

[37] S. Ghosal, H. Luitel, S. K. Mandal, D. Sanyal, D. Jana, Half metallic ferromagnetic and optical properties of ruthenium-doped zincblende ZnS: A first principles study, *Journal of Physics and Chemistry of Solids*, 136 (2020) 109175.

[38] S. H. Saberi, S. M.Baizaee, H. Kahnouji, Electronic structure and magnetic properties of transition-metal (Y, Zr, Nb, Mo, Tc, Ru, Rh, Pd, Ag and Cd) doped in GaN nanotubes, *Superlattices and Microstructures*, 74 (2014) 52-60.

[39] P. Hohenberg, W. Kohn, Inhomogeneous Electron Gas, *Physical Review*, 136(3B) (1964) B864.

[40] W. Kohn, L. J. Sham, Self-Consistent Equations Including Exchange and Correlation Effects, *Physical Review*, 140(4A) (1965) A1133.

[41] P. Giannozzi, S. Baroni, N. Bonini, M. Calandra, R. Car, C. Cavazzoni, D. Ceresoli, G. L.Chiarotti, M. Cococcioni, I. Dabo, A. D. Corso, S. Fabris, G. Fratesi, S. D. Gironcoli, R. Gebauer, U. Gerstmann, C. Gougoussis, A. Kokalj, M. Lazzeri, L. M. Samos, N. Marzari, F. Mauri, R. Mazzarello, S. Paolini, A. Pasquarello, L. Paulatto, C. Sbraccia, S. Scandolo, G. Sclauzero, A. P. Seitsonen, A. Smogunov, P. Umari, R. M Wentzcovitch, QUANTUM ESPRESSO: a modular and open-source software project for quantum simulations of materials, *Journal of Physics: Condensed Matter*, 21(39) (2009) 395502.

[42] P. Giannozzi, O. Andresussi, T. Brumme, O. Bunau, M. B. Nardelli, M. Calandra, R. Car, C. Cavazzoni, D. Ceresoli, M. Cococcioni, A. D. Corso, S. D,Gironcoli, P. Delugas, R. A.Distasio Jr, A. Ferretti, A. Floris, G. Fratesi, G. Fugallo, R. Gebauer,U. Gerstmann, F. Giustino,

16

T. Gorni, J. Jia, M. Kawamura, H. Y. Ko, A. Kokalj, E.Kũcũkbenli, M. Lazzerri, M. Marsili, N. Marzari, F. Mauri, N. L. Nguyen, A. O. D. L. Roza, L. Paulatto, S. Poncè, D. Rocca, R. Sabatini, B. Santra, M. Schlipf, A. P. Seitsonen, A. Smogunov, I. Timrov, T. Thonhauser, P. Umari, N. Vast, X. Wu, S. Baroni, Advanced capabilities for materials modelling with Quantum ESPRESSO,*Journal of physics: Condensed matter*, 29(46) (2017) 465901.

[43] P. Giannozzi, O. Baseggio, P. Bonfa, D. Brunato, R. Car, I. Carnimeo, C. Cavazzoni, S. de Gironcoli, P. Delugas, F. Ferrari Ruffino, A. Ferretti, N. Marzari, I. Timrov, A. Urru, S. Baroni, Quantum ESPRESSO toward the exascale, *Journal of Chemical Physics*, 152 (2020) 154105.

[44] J. P. Perdew, K. Burke, M. Ernzerhof, Generalized Gradient Approximation Made Simple, *Physical Review Letters*, 77(18) (1996) 3865.

[45] H. J. Monkhorst, J. D. Pack, Special points for Brillouin-zone integrations, *Physical Review B*, 13(12) (1976) 5188.

[46] N. Marzari, D. Vanderbilt, A. De Vita, M. C. Payne, Thermal Contraction and Disordering of the Al(110) Surface, *Phys. Rev. Lett.*, 82 (1999) 3296.

[47] H. M. Ghaitan, Z. A. Alahmed, S. M. H. Qaid, M. Hezam, A. Aldwayyan, Density Functional Study of Cubic, Tetragonal, and Orthorhombic CsPbBr$_3$ Perovskite, *ACS Omega*, 5(13) (2020) 7468-7480.

[48] A. Yoshikawa, E. Ohshima, T. Fukuda, H. Tsuji, K. Oshima, Crystal growth of GaN by ammonothermal method, *Journal of Crystal Growth*, 260(1-2) (2004) 67-72.

[49] K. Karch, J. M. Wagner, F. Bechstedt, Ab initio study of structural, dielectric, and dynamical properties of GaN, *Physical Review B*, 57(12) (1998) 7043.

[50] B. Doumi, A. Tadjer, F. Dahmane, D. Mesri, H. Aourag, Investigations of structural, electronic, and half-metallic ferromagnetic properties in $(Al, Ga, In)_{1-x}M_xN$ (M=Fe, Mn) Diluted Magnetic Semiconductors, *Journal of Superconductivity and Novel Magnetism*, 26(3) (2013) 515-525.